

RESPONSE OF REINFORCED CONCRETE PILES INCLUDING SOIL-PILE INTERACTION EFFECTS

S. Limkatanyu¹, K. Kuntiyawichai², E. Spacone³, and M. Kwon⁴

¹Assistant Professor, Dept. of Civil Engineering, Faculty of Engineering, Prince of Songkla University, Songkhla, Thailand

²Assistant Professor, Dept. of Civil Engineering, Faculty of Engineering, Ubonratchathani University, Ubonratchathani, Thailand

³Professor, PRICOS Department, University of Chieti, Pescara, Italy

⁴Associate Professor, Dept. of Civil Engineering, Gyeongsang National University, Gyeongnam, Korea

Email: suchart.l@psu.ac.th, kittisak.ubu@gmail.com, espacone@unich.it, and kwonm@nongae.gsnu.ac.kr

ABSTRACT :

Due to recent destructive earthquakes, the lateral behaviors of pile foundations have been extensively investigated through experimental and numerical studies. The main objective of this work is to develop the frame model with lateral deformable supports for pile-soil systems under cyclic lateral loadings. This proposed model is simple and computational efficient but capable of representing the salient features of pile-soil systems under cyclic lateral loadings; including dragging force and gap formation along the pile-soil interfaces as well as hysteretic responses of surrounding soils and piles. The accuracy of the proposed model is verified through correlation studies on full scale tests of Cast-In-Drilled-Hole (CIDH) piles partially embedded in cohesionless soil. Results from these correlation studies indicate that the proposed model can represent well both on global and local hysteretic responses.

KEYWORDS: Soil-Structure Interaction, Reinforced Concrete, Piles, Fiber Model, Cyclic Loads, Nonlinear Frame Analysis.

1. INTRODUCTION

Nowadays, both structural and geotechnical engineers are challenged to design and investigate expensive and strategic structures (e.g. high-rise buildings, offshore platforms, multi-story highways etc.) for extreme lateral loadings (e.g. earthquakes, gusty winds, terrorist attacks, etc.). Usually, pile foundations are used to support these structures. Consequently, the inclusion of the soil-pile system into the numerical model is crucial for design and analysis of these structures under extreme events. It is desirable that the pile foundations remain elastic under these extreme loadings. Such desire is to avoid the difficulties of subsurface inspection and high cost of repairing the foundation damage. Nevertheless, the bending moment induced by the design seismic activity can be adequately large to cause flexural damage in the pile. Post earthquake investigations in recent earthquakes have confirmed that pile foundations are prone to flexural damages from earthquake loadings [1]. The flexural damages in pile foundation can reduce both stiffness and strength of the foundation; hence affecting its serviceability and existing loading-capacity of the structural system. Furthermore, it is imperative to consider the effects of soil-foundation system on seismic demand and structural response when the performance-based methodology is used in seismic design of structures.

The main objectives of this paper are to present the newly developed pile-soil frame element and to assess the validity of the proposed model through correlation studies on full scale tests on piles under lateral loadings. The formulation of the pile-soil frame element is based on the principle of virtual displacements. The so-called "Winkler Foundation" is employed to represent the surrounding soils [2]. Furthermore, it is crucial to note that this study emphasizes only on soil-pile interaction in firm non-liquefiable soil induced by the inertia of the superstructures (inertial interaction). Kinematic interaction related to scattering of incoming seismic waves and effects of soil liquefaction are not included in this study.

Finally, the experimental data on full scale tests of Cast-In-Drilled-Hole (CIDH) piles partially embedded in cohesionless soil is used to assess the accuracy of the proposed model. Both global and local responses of the system are evaluated. It is noted that this foundation type is frequently used as supporting systems of highway bridges, especially in California. The main advantage of this pile construction is the cost saving associated with the construction of one large CIDH pile instead of multiple smaller diameter driven piles, which must be integrated through a pile-cap.

2. DISPLACEMENT-BASED FIBER FRAME ELEMENT WITH LATERAL DEFORMABLE SUPPORTS

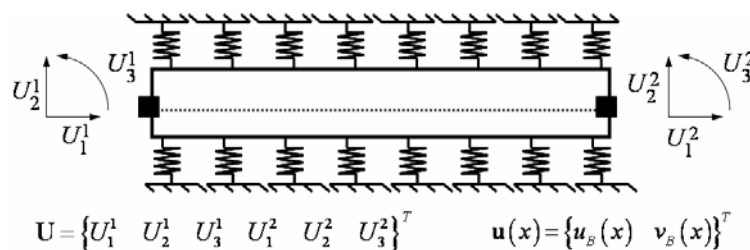


Figure 1 2-Node displacement-based fiber frame element with lateral deformable supports

The 2-node displacement-based frame element with lateral deformable supports (e.g. soil) is shown in Fig. 1. The interactions between the frame and surrounding deformable medium are represented by continuous lateral springs. The proposed frame element with lateral deformable supports is made of the following components: a 2-node frame, plus continuous lateral springs representing the surrounding deformable medium. The frame section is discretized into fibers. The element nodal displacements \mathbf{U} and the section displacements $\mathbf{u}(x)$ are also indicated in Fig. 1. The section deformations are grouped in the $\mathbf{d}_B(x) = \{\varepsilon_B(x) \quad \kappa_B(x)\}^T$ where $\varepsilon_B(x)$ is the section axial strain and $\kappa_B(x)$ is the section curvature. The frame formulation is based on the Euler-Bernoulli beam theory, neglecting the section shear deformation. Based on the small deformation assumption, the section deformations are related to the nodal displacements through the compatibility relations

$\varepsilon_B = du_B/dx$ and $\kappa_B = dv_B^2/dx^2$. The section forces conjugate of $\mathbf{d}_B(x)$ are $\mathbf{D}_B(x) = \{N_B(x) \ M_B(x)\}^T$, where $N_B(x)$ and $M_B(x)$ are the frame section axial load and bending moment, respectively. The element displacements $\mathbf{u}(x)$ are expressed as functions of the nodal displacements \mathbf{U} through the shape functions $\mathbf{N}_B(x)$:

$$\mathbf{u}(x) = \mathbf{N}_B(x)\mathbf{U} \quad (2.1)$$

where $\mathbf{N}_B(x)$ is the array containing the shape functions of a two-node frame. They are well-established functions that define a linear axial displacement field and a cubic vertical displacement field. Frame and lateral-support compatibility are both enforced in the strong form. The section and lateral-support deformations are directly related to the nodal displacements \mathbf{U} through the following equations:

$$\mathbf{d}_B(x) = \mathbf{B}_B(x)\mathbf{U}; \quad \mathbf{d}_s(x) = \mathbf{B}_s(x)\mathbf{U} \quad (2.2)$$

where $\mathbf{B}_B(x) = \partial_B \mathbf{N}_B(x)$, $\mathbf{B}_s(x) = \partial_s \mathbf{N}_B(x)$; ∂_B and ∂_s are linear differential operators.

Element equilibrium is enforced in the weak form. Application of the principle of virtual displacements, substitution of Eqn. 2.2 and subsequent elimination of the virtual nodal displacements $\delta\mathbf{U}$, yield the following equilibrium statement:

$$\int_L \mathbf{B}_B^T(x) \mathbf{D}_B(x) dx + \int_L \mathbf{B}_s^T(x) \mathbf{D}_s(x) dx = \mathbf{P} \quad (2.3)$$

where \mathbf{P} is the nodal force vector conjugate of \mathbf{U} ; and $\mathbf{D}_s(x)$ contains the lateral-support forces. If Eqn. 2.3 is rewritten in incremental form, the matrix form of element equilibrium becomes:

$$\mathbf{K} \Delta\mathbf{U} = \mathbf{P} - \mathbf{P}^0 \quad (2.4)$$

where \mathbf{K} is the element stiffness matrix, computed as:

$$\mathbf{K} = \mathbf{K}_B + \mathbf{K}_s \quad (2.5)$$

where \mathbf{K}_B and \mathbf{K}_s are the frame and the lateral-support contributions to the element stiffness, respectively.

$$\mathbf{K}_B = \int_L \mathbf{B}_B^T(x) \mathbf{k}_B \mathbf{B}_B(x) dx; \quad \mathbf{K}_s = \int_L \mathbf{B}_s^T(x) \mathbf{k}_s \mathbf{B}_s(x) dx \quad (2.6)$$

$\mathbf{k}_B(x)$ is the frame section stiffness and $\mathbf{k}_s(x)$ is the lateral-support stiffness. \mathbf{P} is the array containing the element forces:

$$\mathbf{P} = \mathbf{P}_B + \mathbf{P}_s \quad (2.7)$$

and $\mathbf{P}^0 = \mathbf{P}_B^0 + \mathbf{P}_s^0$ is the array containing the element initial forces. \mathbf{P}_B is the frame contribution to the element forces, and \mathbf{P}_s is the contribution of the lateral supports:

$$\mathbf{P}_B = \int_L \mathbf{B}_B^T(x) \mathbf{D}_B(x) dx; \quad \mathbf{P}_s = \int_L \mathbf{B}_s^T(x) \mathbf{D}_s(x) dx \quad (2.8)$$

The details of this model formulation can be found in Limkatanyu and Spacone [3]. The general-purpose finite element program [4] is used to host this proposed element.

3. MONOTONIC AND CYCLIC $p-y$ CURVES of COHESIONLESS SOILS

In this study, the soils surrounding a pile are modeled as 1-D springs continuously placed along the pile length. Only the end-bearing pile embedded in cohesionless soil is considered in this study. Based on the model proposed by Reese et al. [5], the ultimate lateral resistance p_u of soils with depth can be computed from the lesser value provided by Eqns. 3.1 and 3.2.

$$p_u = \gamma z \left[\begin{array}{l} D(K_p - K_a) + z(K_p - K_0) \sqrt{K_p} \tan \alpha \\ + zK_0 \sqrt{K_p} \left(\frac{1}{\cos \alpha} + 1 \right) \tan \phi' \sin \beta \end{array} \right] \quad (3.1)$$

$$p_u = \gamma z D (K_p^3 + K_0 K_p^2 \tan \phi' - K_0) \quad (3.2)$$

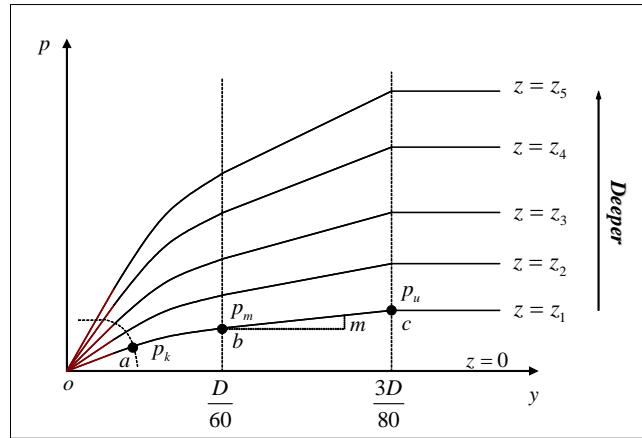


Figure 2 Monotonic backbone p - y curves of sand proposed by Reese et al [5].

where $K_p = \tan^2(45^\circ + \phi'/2)$ is passive earth pressure coefficient; $K_a = \tan^2(45^\circ - \phi'/2)$ is active earth pressure coefficient; K_0 is at-rest earth pressure coefficient; ϕ' is effective internal friction angle; $\alpha = \phi'/2$ is angle defining the shape of failure wedge; $\beta = 45^\circ + \phi'/2$; γ is the effective unit weight of soil; z is depth from the ground surface; and D is the pile diameter. It is noted that Eqn. 3.1 accounts for the wedge-type failure near the surface while Eqn. 3.2 accounts for the plane-strain failure at a great depth below the ground surface. The monotonic backbone p - y curves relating the soil deformation to soil pressure are shown in Fig. 2 at various depths.

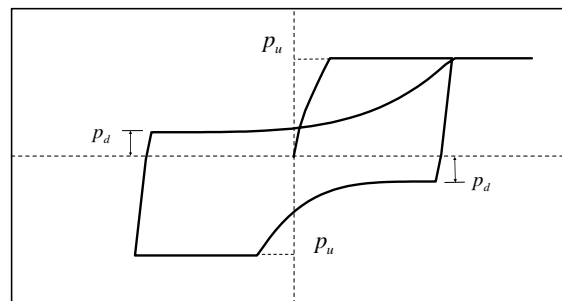


Figure 3 Cyclic response of sand

The monotonic p - y curve of Fig. 2 serves as the envelope of the cyclic p - y curve as shown in Fig. 3. The hysteretic characteristic of the model developed by Arnold et al. [6] is modified for the proposed cyclic p - y model. This proposed model can account for gapping and dragging aspects observed during in-situ tests on piles under cyclic lateral loadings (e.g. Brown et al. [7]). The dragging force is activated only when the pile moves through the gap. The value of the dragging resistance is taken as 30 % of the monotonic peak capacity as suggested by Hutchinson et al. [8].

4. CORRELATION STUDIES ON CAST-IN-DRILLED-HOLE PILE FOUNDATION UNDER LATERAL CYCLIC LOADINGS

The frame element with lateral deformable supports discussed above is employed to simulate both global and local responses of the pile-soil systems under lateral loadings. The fiber section model is used to describe the responses of the pile section. In this study, the fiber section is consisted of 400 confined concrete fibers, 100

unconfined concrete fibers, and 7 steel fibers. The uniaxial constitutive library developed by Limkatanyu [9] is used to model the hysteretic response of each constituent fiber.

In this paper, one of the experimental data from a series of full-scale CIDH pile tests by Chai and Hutchinson [10] is used to evaluate the validity of the proposed frame model. This pile is labeled as Chai-Hutchinson Pile #1. More results of correlation studies on this test series are presented elsewhere [11]. The geometry of this specimen is shown in Fig. 4. The pile was subjected to a constant axial compression of 489 kN (corresponding to approximately 10 % $f_c' A_g$) and a cyclic lateral tip-displacement as shown in Fig. 5. The material properties of concrete, reinforcing steel, and surrounding sands were taken from the report by Chai and Hutchinson [10].

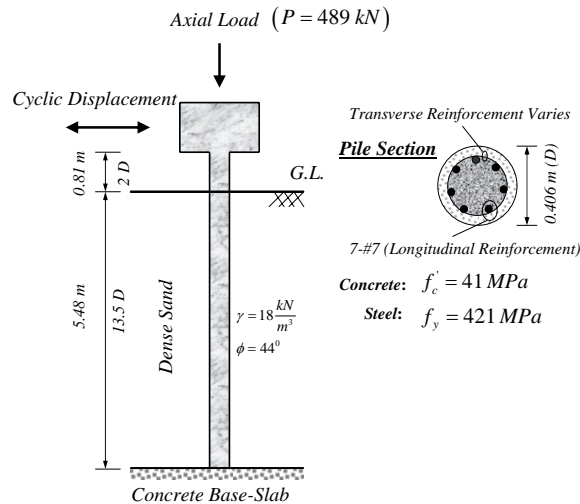


Figure 4 Geometry and loads of Chai-Hutchinson Pile #1

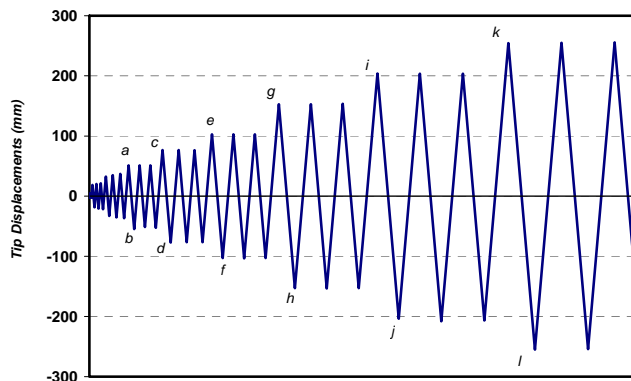


Figure 5 Tip displacement history of Chai-Hutchinson Pile #1

Fig. 6 (a) superimposes the tip load-displacement response from the experimental test with the numerical result obtained with the proposed model without dragging-gapping effects while Fig. 6 (b) compares the experimental results with the numerical result obtained with the proposed model with dragging-gapping effects. As expected, both models yield the same strength. This is due to the fact the ultimate soil pressures of both models are computed based on Eqns. 3.1 or 3.2. Negligence of dragging-gapping effects can result in over-prediction of the hysteretic energy of the system. It is clear that the proposed model with dragging-gapping effects could represent well the initial stiffness and the peak lateral load, which is essential for the overall strength of the structural system. Furthermore, the proposed model with dragging-gapping effects could also represent well the hysteretic features of the system such as unloading-reloading branches, post-peak strength degradation, and the hysteretic energy dissipated during the loading cycles.

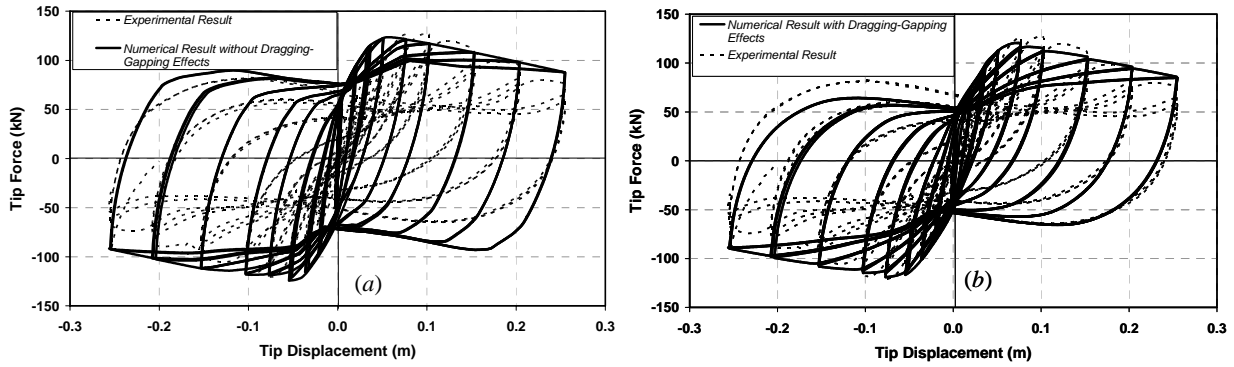


Figure 6 Experimental and numerical responses of Chai-Hutchinson Pile #1

Fig. 7 shows the lateral displacement profiles of the pile at different loading cycles (the cycle numbers refer to the labeling of Fig. 5). The clear-cut changes in the slope of displacement profiles are observed. These are associated with the plastic-hinge formation, especially for large displacement cycles. The lateral deflections are rather small beyond the plastic-hinge region; implying that the inelastic deformation of the pile is localized only within upper few diameters of the pile. When comparing the left (Fig. 7 (a)) and right (Fig. 7 (b)) deflection profiles, one could observe the distinct features of these two deflection directions. The gap formation along the left deflection trends to be larger than that along the right deflection. This feature was also observed during the test by Chai and Hutchinson [10]. Furthermore, it is interesting to note that this feature was not found when the dragging-gapping effects were not included in the numerical model.

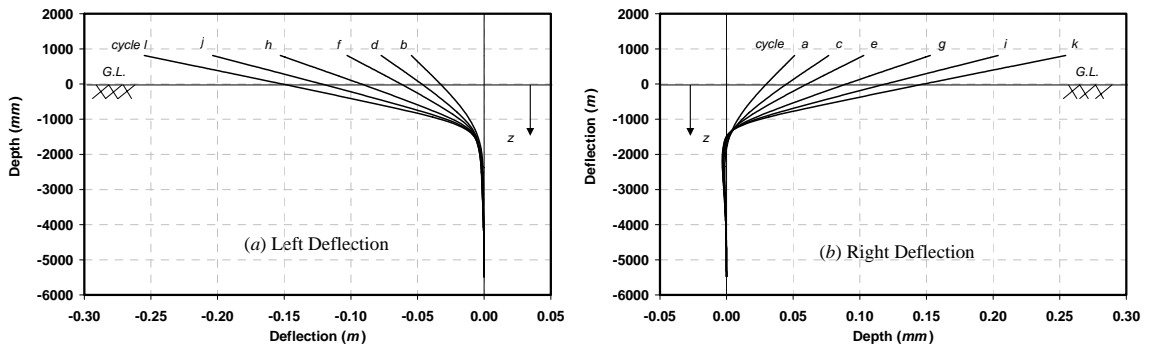


Figure 7 Lateral displacement profiles at different cycles: (a) left deflection; (b) right deflection

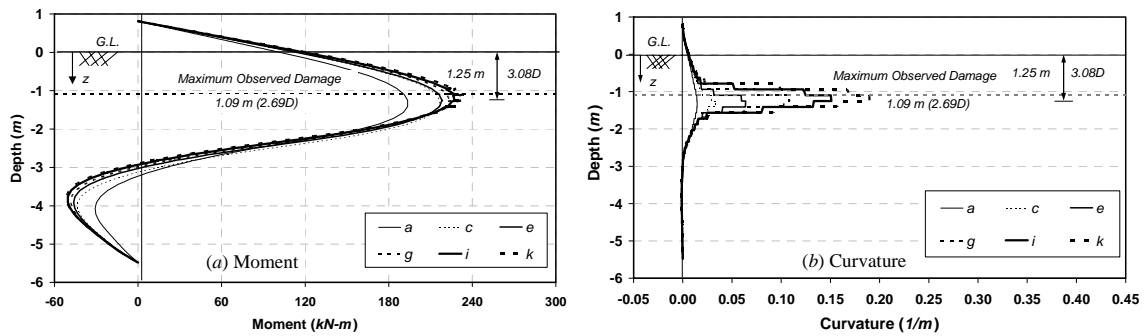


Figure 8 Moment and curvature profiles at different cycles

Fig. 8 (a) and (b) show the moment and curvature profiles of the pile at different loading cycles (the cycle numbers refer to the labeling of Fig. 5). As shown in Fig. 8, the depth-to-maximum moment (plastic-hinge location) obtained with the proposed model is 1.25 m (3.08 D). This value is complied well with the test observation of maximum damage to the pile at 1.09 m (2.69 D).

Fig. 9 shows the hysteretic responses of surrounding soils at various depths. These responses confirm that the dragging and gapping effects should be considered in order to appropriately cope with the problem of cyclic soil-pile interaction.

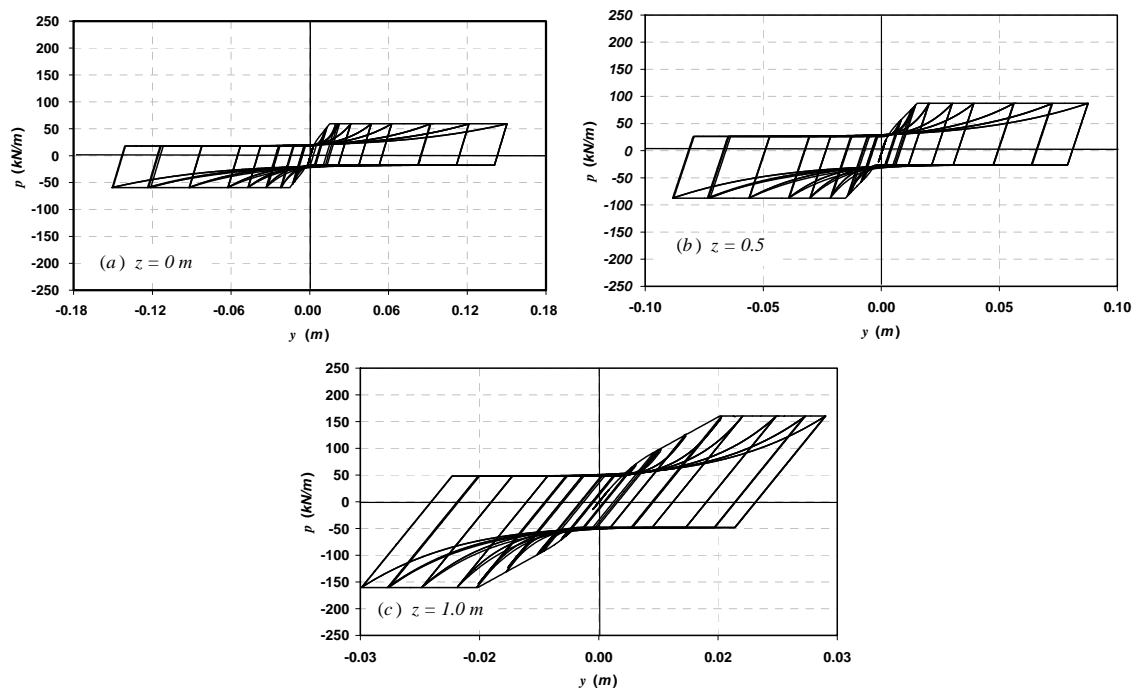


Figure 9 Cyclic p - y responses at various depths

5. CONCLUSIONS

In this study, the simplified model for analysis of single pile-soil system is proposed. This model is a displacement-based frame fibre element with continuous lateral deformable supports. The so-called “*Winkler Foundation*” is employed to represent the response of the surrounding soils. The proposed model can account for dragging force and gap formation along the pile-soil interfaces as well as hysteretic responses of surrounding soils and pile.

Experimental data from a full scale test of the CIDH pile under cyclic lateral loading are used to evaluate the ability of the proposed model. The correlation studies indicate that the proposed model is capable of predicting both global and local responses of the pile-soil system despite the use of rather simple one-dimensional p - y springs to represent the surrounding soils. This enhances the confidence on accounting for effects of soil-foundation system on seismic demand and structural response especially when the performance-based methodology is used in seismic design of structures.

6. ACKNOWLEDGEMENTS

This study was partially supported by the Thai Ministry of University Affairs (MUA), by the Thailand Research Fund (TRF) under Grant MRG4680109, by the National Science Foundation under Grant No. CMS-0010112 by the Italian Ministry of Education, University and Research (MIUR) under Cofin 2002 and 2004 Grants, and by STREAM Research Group. This support is gratefully acknowledged. Any opinions expressed in this paper

are those of the authors and do not reflect the views of the sponsoring agencies. The authors would also like to thank Prof. Y. H. Chai of the University of California, Davis and Prof. T.C. Hutchinson of the University of California, San Diego for providing the experimental data used in this paper. Special thanks go to Dr. Passagorn Chaiviriyawong for his fruitful discussion on the theoretical aspects.

REFERENCES

- [1] Sitar, N. (1995). Geotechnical Reconnaissance of the Effects of the January 17, 1995 Hyogoken-Nambu Earthquake, Japan, *UCB/EERC 95/01 Earthquake Engineering Research Center*, University of California, Berkeley, California.
- [2] Winkler, E. (1867). *Theory of Elasticity and Strength*. H. Dominicus, Prague.
- [3] Limkatanyu, S. and Spacone, E. (2006). Frame element with lateral deformable supports: formulations and numerical validation. *Computers and Structures*. 84, no. 13-14, 942-954.
- [4] Taylor, R.L. (2000). FEAP: Finite Element Analysis Program. Department of Civil and Environmental Engineering, University of California, Berkeley, California.
- [5] Reese, L.C., Cox, W.R., and Koop, F.D. (1974). Analysis of laterally loaded piles in sand, *The 6th Offshore Technology Conference*, Houston, Texas.
- [6] Arnold, P., Bea, R.G., Idriss, I.M., Reimer, R.B., Beebe, K.E. and Marshall, P.W. (1977). Study of soil-pile-structure systems in severe earthquakes, *Proceedings of the Annual Offshore Technology Conference*, Houston, Texas.
- [7] Brown, D.A., Morrison, C., and Reese, L.C. (1988). Lateral load behavior of pile group in sand, *Journal of Geotechnical Engineering*. 114, no. 11, 1261-1276.
- [8] Hutchinson, T.C., Chai, Y.H., and Boulanger, R.W. (2005). Simulation of full-scale cyclic lateral tests on piles, *Journal of Geotechnical and Geoenvironmental Engineering*. 131, no. 9, 1172-1175.
- [9] Limkatanyu, S. (2004). Deformation-based uniaxial constitutive library for the inelastic analysis of RC structures: fiber section and beam column element, *The 7th International Conference on Concrete Technology*, Kuala Lumpur, Malaysia.
- [10] Chai, Y.H. and Hutchinson, T.C. (1999). Flexural Strength and Ductility of Reinforced Concrete Bridge Piles. UCD-STR 99/02. Department of Civil and Environmental Engineering, University of California, Davis, California.
- [11] Limkatanyu, S., Kuntiyawichai, K., and Spacone, E. (2008). Responses of reinforced concrete piles including soil-pile interaction effects, *Engineering Structures* (Under Review).